

Rotational correlation and dynamic heterogeneity in a kinetically constrained lattice gas

Albert C. Pan

Department of Chemistry, University of California, Berkeley, CA 94720-1460

(Dated: November 24, 2017)

We study dynamical heterogeneity and glassy dynamics in a kinetically constrained lattice gas model which has both translational and rotational degrees of freedom. We find that the rotational diffusion constant tracks the structural relaxation time as density is increased whereas the translational diffusion constant exhibits a strong decoupling. We investigate distributions of exchange and persistence times for both the rotational and translational degrees of freedom and compare our results on the distributions of rotational exchange times to recent single molecule studies.

I. INTRODUCTION

Glassformers are dynamically heterogeneous. Neighboring regions, nanometers in size, can have local relaxation times which differ by several orders of magnitude [1, 2]. Experimental measures of heterogeneous dynamics often probe rotational degrees of freedom. For example, Deschenes and Vandembout [2, 3] have measured the rotation of single probe molecules in a polymer film near the glass transition. Here, we investigate a kinetically constrained lattice gas model with translational and rotational degrees of freedom which captures many of the essential features seen in these experiments such as stretched exponential decay of rotational autocorrelation functions as temperature is decreased and heterogeneous distributions of exchange times.

In section II, we present the model and the computational methods used. Section III demonstrates the existence of heterogeneous dynamics. We also present ensemble measurements which display a precipitous dynamical slowdown and breakdown of mean field dynamical relations. Section IV measures distributions of persistence and exchange times. Finally, section V compares these distributions to those observed recently in single molecule studies.

II. MODELS AND COMPUTATIONAL DETAILS

One route to understanding dynamical heterogeneity relies on the presence of local steric constraints on the movement of particles which make themselves felt to an increasing degree as temperature is lowered (or density is increased). The kinetically constrained lattice gas models [4] are simple caricatures of glassformers which employ local steric constraints as their sole means to glassiness in the absence of any non-trivial static correlations between particles. It has been shown that, despite their apparent simplicity, these models exhibit surprisingly many of the hallmarks of glassy behavior that have been the focus of recent experimental and theoretical efforts [4, 5, 6, 7, 8]. The model we study consists of hard core particles on a triangular lattice with no static interactions other than those that prohibit multiple occupancy of a single site. To each particle is associated a vector which can point along the six directions bisecting the triangular lattice. In other words, the vectors point toward the interstitial sites of the lattice [9].

Translation of particles obeys the kinetic constraints of the two vacancy assisted triangular lattice gas, or the (2)-TLG [10, 11]: a particle at site \mathbf{r} is allowed to move to a nearest neighbor site, \mathbf{r}' , if (1) \mathbf{r}' is not occupied and (2) the two mutual nearest neighbor sites of \mathbf{r} and \mathbf{r}' are also empty. These rules coincide with a physical interpretation of steric constraints on the movement of hard core particles in a dense fluid [10].

Rotation of particles obeys a similarly physically motivated kinetic constraint if one imagines that the particles have small hard protrusions along the direction of their orientation vector [9]: a particle, i , with a unit vector \mathbf{p}_i , can rotate either 60 degrees clockwise or counterclockwise provided the two neighboring lattice sites along the direction between the initial and final orientations of \mathbf{p}_i are empty. Translations preserve the direction of \mathbf{p}_i . We refer to this model as the rotational TLG [9]. Due to the absence of non-trivial static interactions, there are no static correlations between particles. However, constraints on the kinetics allow non-trivial dynamic correlations to emerge in trajectory space.

In the computer simulations, we investigated particle densities, ρ , between 0.10 and 0.81 on a lattice with edge length $L = 128$ ($L = 256$ for $\rho = 0.81$). The density $\rho = 1$ corresponds to the completely full lattice. At densities up to and including 0.77, over 60 independent trajectories of lengths 10-100 times τ_α , where τ_α is the time for the self-intermediate scattering function at $\mathbf{q} = (\pi, 0)$ [12] to reach $1/e$ of its initial value (see below), were run. At densities 0.79, 0.80 and 0.81, four to sixteen trajectories were run. These trajectories were stored logarithmically for later analysis (i.e. configurations were saved after 1, 2, 4, 8, 16, 32, etc. sweeps). Time was measured in Monte Carlo sweeps. During each sweep, particles were chosen randomly and translational and orientational moves were attempted

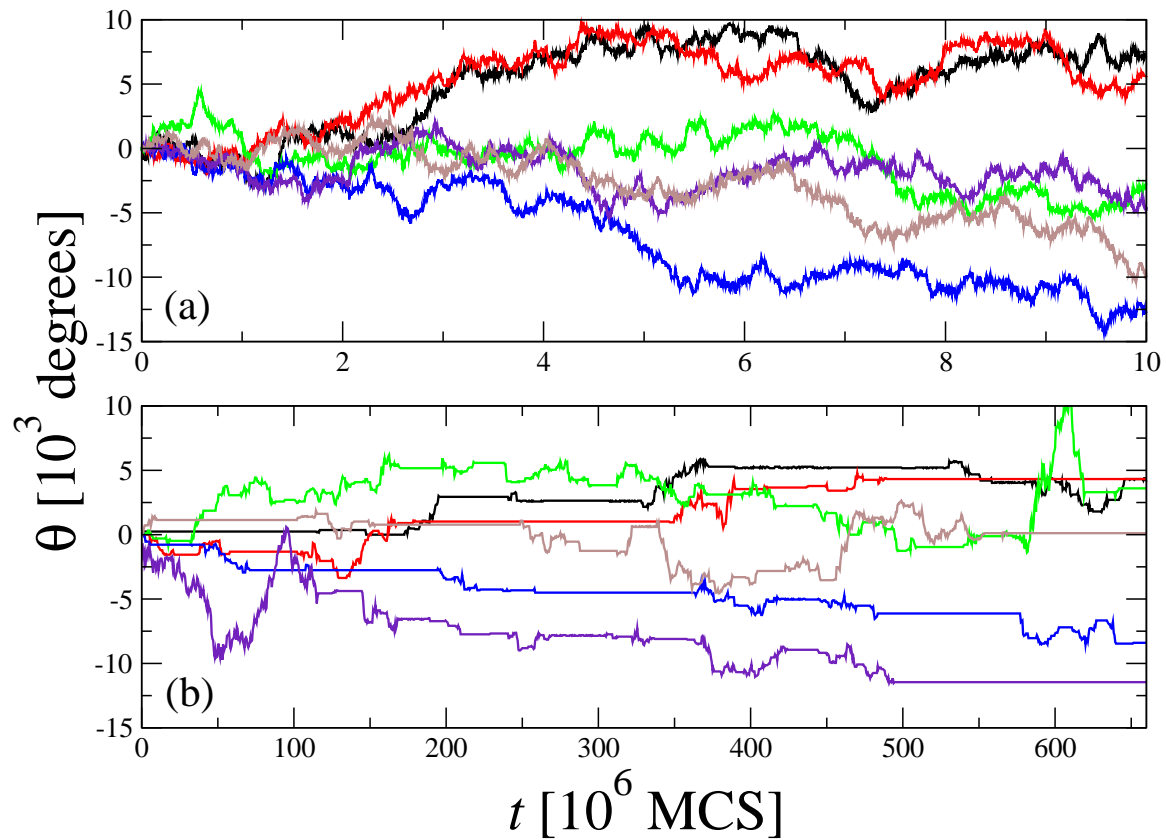


FIG. 1: Rotational trajectories of single particles at (a) low density ($\rho = 0.30$) and (b) high density ($\rho = 0.77$).

with equal probability. For the higher density runs, a continuous time algorithm was used for greater efficiency [13]. This algorithm involved making and updating a list of only those particles which have the possibility of either moving or rotating and choosing from among those exclusively during every move. The time was then incremented as one over the number of possible moves. Due to the lack of static correlations, initial configurations could be generated by random occupation of empty lattice sites by particles with random orientations until the desired density was reached.

III. HETEROGENEOUS DYNAMICS AND ROTATIONAL CORRELATION TIMES

Despite the lack of static correlations between rotational and translational degrees of freedom, dynamic coupling exists via the kinetic constraints [9]. A particle which cannot rotate because it is sterically blocked by neighboring particles must wait for those particles to translate away before it is allowed to rotate again. In this sense, we expect rotational dynamics to be a good indicator of local structural relaxation in this model, as they are in experiment.

Fig. 1 shows rotational trajectories of six particles at low and high densities. The particles at low density (Fig. 1a) rotate freely, performing a random walk through all angles. At higher densities, the particles perform random walks punctuated by periods of little to no rotation. In contrast to the trajectories at low density, dynamics at high density are clearly heterogeneous: at any given time, some particles are rotating quickly while others are essentially frozen. Similar behavior has been observed for translational motion of a probe molecule immersed in spin-facilitated models [14, 15] and in polymer films [2, 3].

A useful ensemble measure of slow dynamics is the rotational autocorrelation function, $C_r(t) = \langle \mathbf{p}_i(0) \cdot \mathbf{p}_i(t) \rangle$, which indicates the time it takes for a particle to lose memory of its initial spin orientation [2, 9]. Here, the angled brackets denote an average over all particles and times, t . A plot of $C_r(t)$ is shown in Fig. 2a. At low densities, relaxation shows a simple exponential profile. As density increases, the curves become more and more stretched exponential indicative of averaging over multiple relaxation timescales. This stretched exponential decay is what one would expect qualitatively from rotational trajectories such as those depicted in Fig. 1b. An important quantity that can be extracted from $C_r(t)$ is the rotational correlation time, τ_r , which is defined as $C_r(\tau_r) = 1/e$. The inverse of this timescale is the rotational diffusion constant, $D_r = \tau_r^{-1}$.

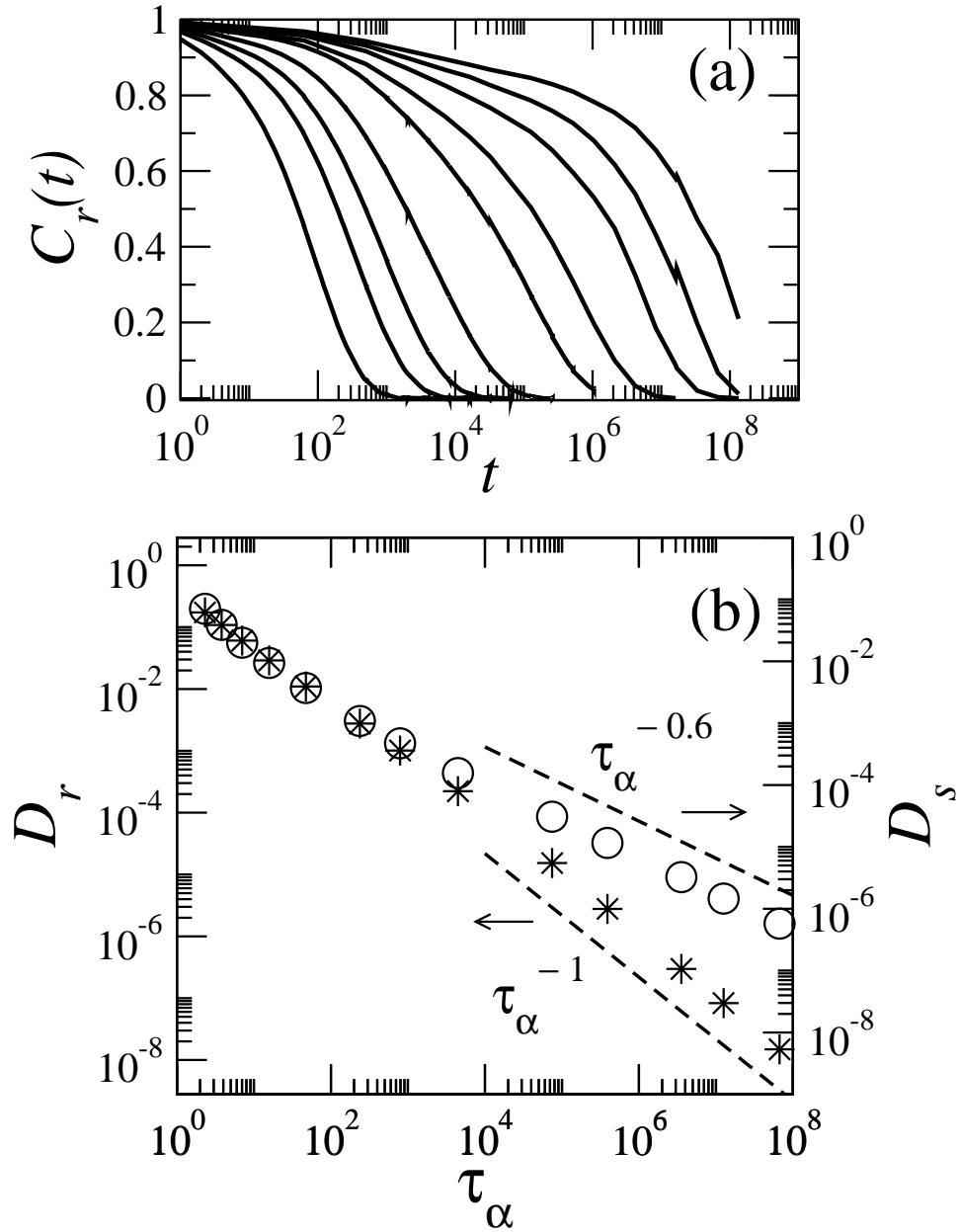


FIG. 2: (a) Rotational autocorrelation at (from left to right) $\rho = 0.50, 0.60, 0.65, 0.70, 0.75, 0.77, 0.79$ and 0.81 . (b) Scaling of the rotational diffusion constant, D_r (stars), and translational self-diffusion constant, D_s (open circles), with structural relaxation time, τ_α . The dashed lines are the power laws, τ_α^{-1} and $\tau_\alpha^{-0.6}$ as indicated.

Translational relaxation is often studied via the self-intermediate scattering function, $F_s(q, t) = \langle e^{i\mathbf{q} \cdot (\mathbf{r}_i(t) - \mathbf{r}_i(0))} \rangle$. Here, $\mathbf{r}_i(t)$ denotes the position of particle i at time t . The decay of the scattering function to $1/e$ at wavevector $\mathbf{q} = (\pi, 0)$ is typically defined to be a structural relaxation time, τ_α , as it gives a sense of how density fluctuations relax at relatively short lengthscales. Dynamic behavior at large lengthscales is studied via the self-diffusion constant, D_s , extracted from the mean-squared displacement, $\langle |\Delta \mathbf{r}_i(t)|^2 \rangle = \langle |\mathbf{r}_i(t) - \mathbf{r}_i(0)|^2 \rangle$. The self-diffusion coefficient, D_s , is defined as $D_s = \lim_{t \rightarrow \infty} \langle |\Delta \mathbf{r}_i(t)|^2 \rangle / 4t$. We omit further discussion of these quantities as they have been presented at length elsewhere for this [6, 10] and other models [8].

An important ramification of heterogeneous dynamics is the breakdown of mean-field dynamical relations such as the much studied Stokes-Einstein (SE) relation [14, 16, 17]. In a system with homogeneous dynamics such as a normal liquid, we expect relaxation behavior to be similar at all but the smallest lengthscales. In a glass, the presence of dynamic heterogeneity implies that such mean-field relations can be violated. In Fig. 2b, we plot the rotational diffusion constant, D_r , and the self-diffusion constant, D_s , versus the translational structural relaxation

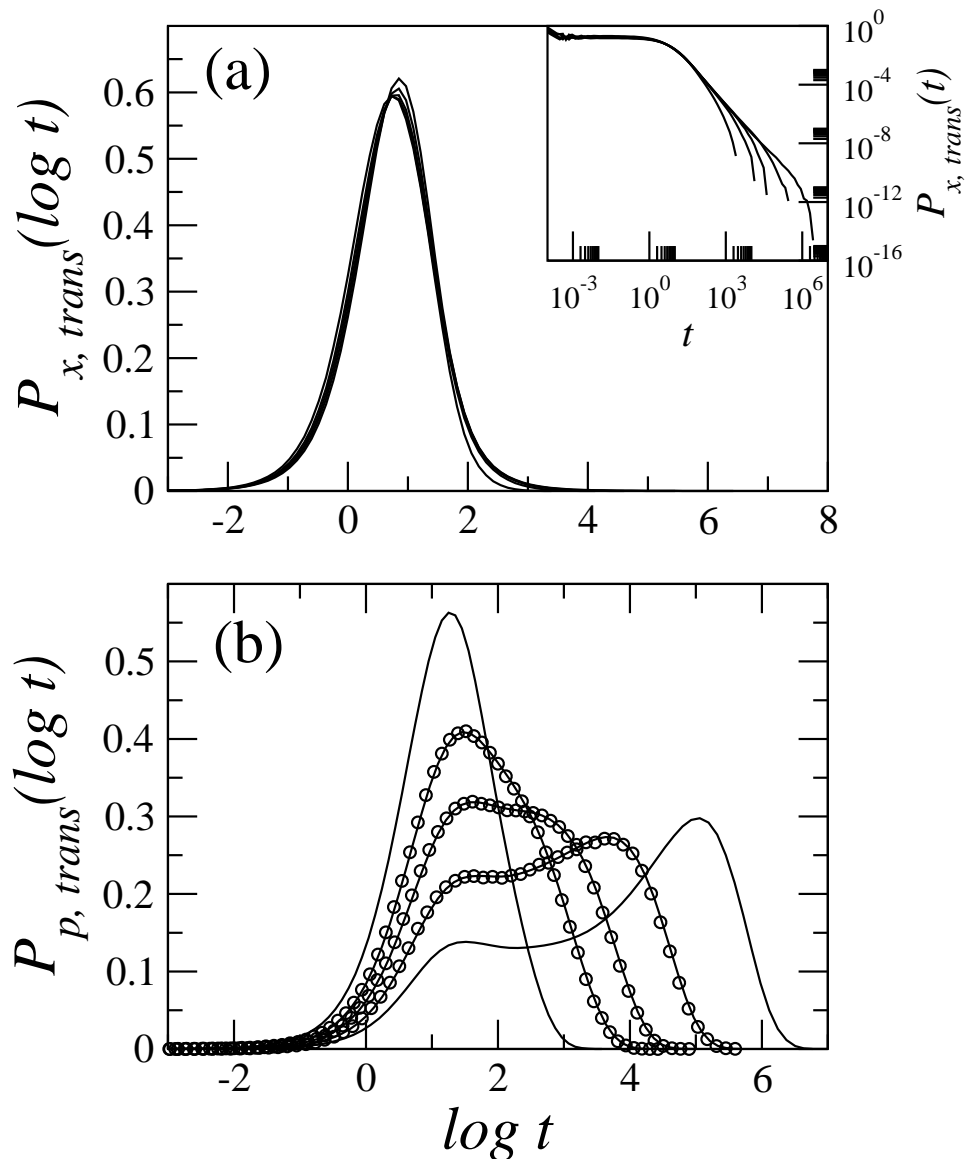


FIG. 3: Distributions of translational (a) exchange and (b) persistence times at (from left to right) $\rho = 0.50, 0.60, 0.65, 0.70$ and 0.75 . The inset to (a) shows the exchange time distributions as a function of linear time, t , as opposed to logarithmic time to emphasize the emergence of broader long time tails as density is increased. The two distributions are related via $P_{x,trans}(\log t) = tP_{x,trans}(t) \ln 10$. The solid lines in (b) are the distributions of persistence times calculated from the distributions of exchange times via eqn. 1 and the open circles are results of direct calculations.

time, τ_α . Rotational diffusion tracks structural relaxation whereas self-diffusion does not. That is, $D_r \sim \tau_\alpha^{-1}$ whereas $D_s \sim \tau_\alpha^{0.6}$. The same trend has been seen in experiment [17]. The scaling of D_r with τ_α can be rationalized qualitatively from the idea mentioned above that the ability to rotate is intimately tied to local structure.

IV. DISTRIBUTIONS OF EXCHANGE AND PERSISTENCE TIMES

Direct measures of heterogeneous dynamics in glassy systems are distribution functions of persistence, $P_p(t)$, and exchange, $P_x(t)$, times [2, 14, 18, 19]. Persistence times measure the first instance of a change in state given an initial configuration. Exchange times measure the duration of particular states. For example, the distribution of rotational persistence times, $P_{p,rot}(t)$, in this model is the distribution of times, given an initial configuration, when a particle changes its rotational state for the first time. The distribution of rotational exchange times, $P_{x,rot}(t)$, is the length of time a particle remains in a particular rotational state. These distributions are multi-point functions because they

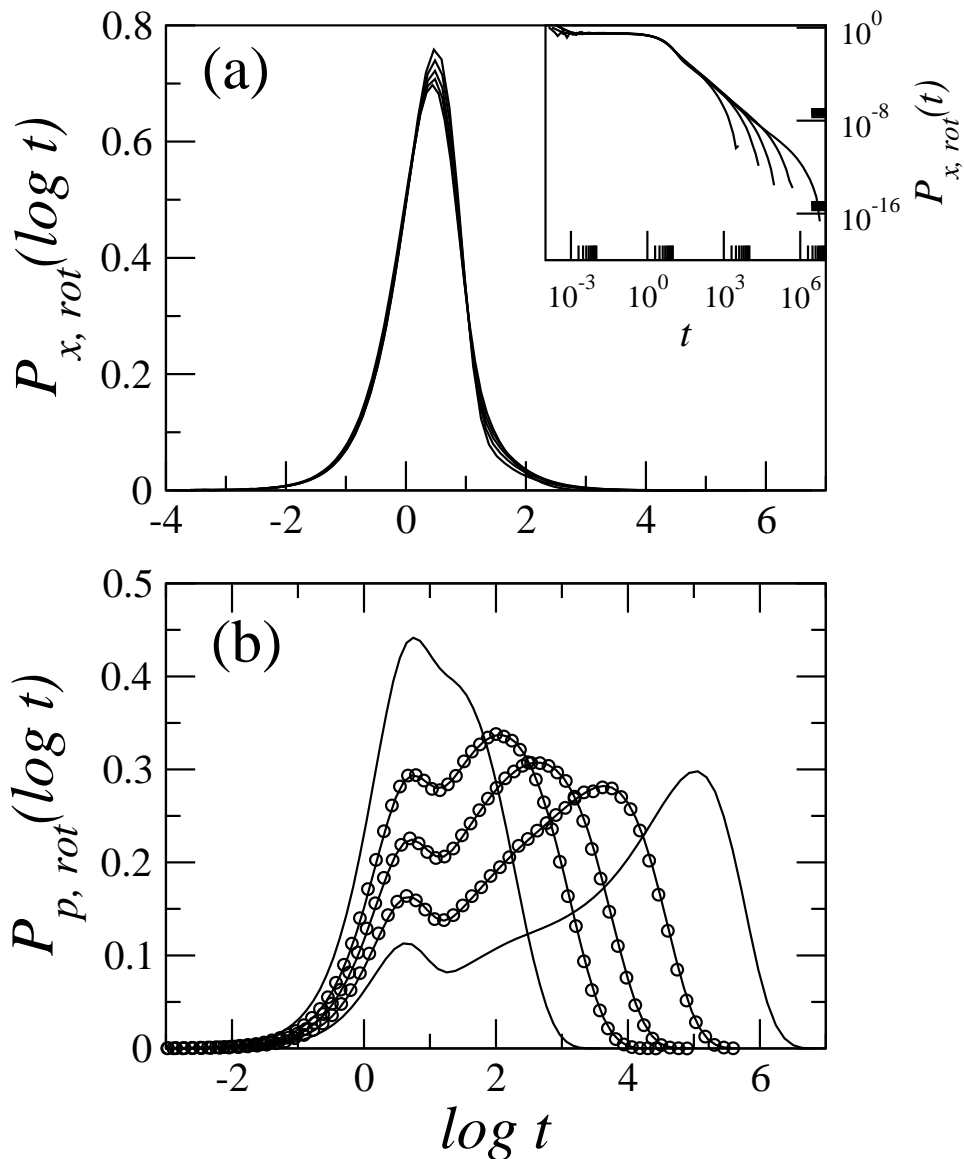


FIG. 4: Same as Fig. 3, except for rotational times.

depend not only on two points in time, but on all intervening points as well. Fig. 3a and Fig. 4a show the distribution of exchange times for translational and rotational motion, respectively. Distributions of exchange times are important for understanding the origin of dynamical decoupling phenomenon [14, 19] (see Fig. 2b).

The distribution of exchange times for translations and rotations are very similar. There is very little change in short time structure as ρ increases. Evidence of broadly distributed dynamics occurs in the long time tails. The distributions of persistence times for translation and rotation are also qualitatively similar and display the same features noted in previous studies [6, 14, 18]. Differences in structure between rotational and translational persistence can be attributed to the differing kinetic constraints. A particle can have the ability to rotate while being constrained translationally and vice versa.

Recently, it has been shown that the distributions of exchange and persistence times are related via the equation [19]:

$$P_p(t) \sim \int_t^\infty P_x(t') dt'. \quad (1)$$

The constant of proportionality is fixed by normalization. This should be a general relation independent of the model or observable studied. The solid lines in Fig. 3b and Fig. 4b show the distribution of persistence times calculated via

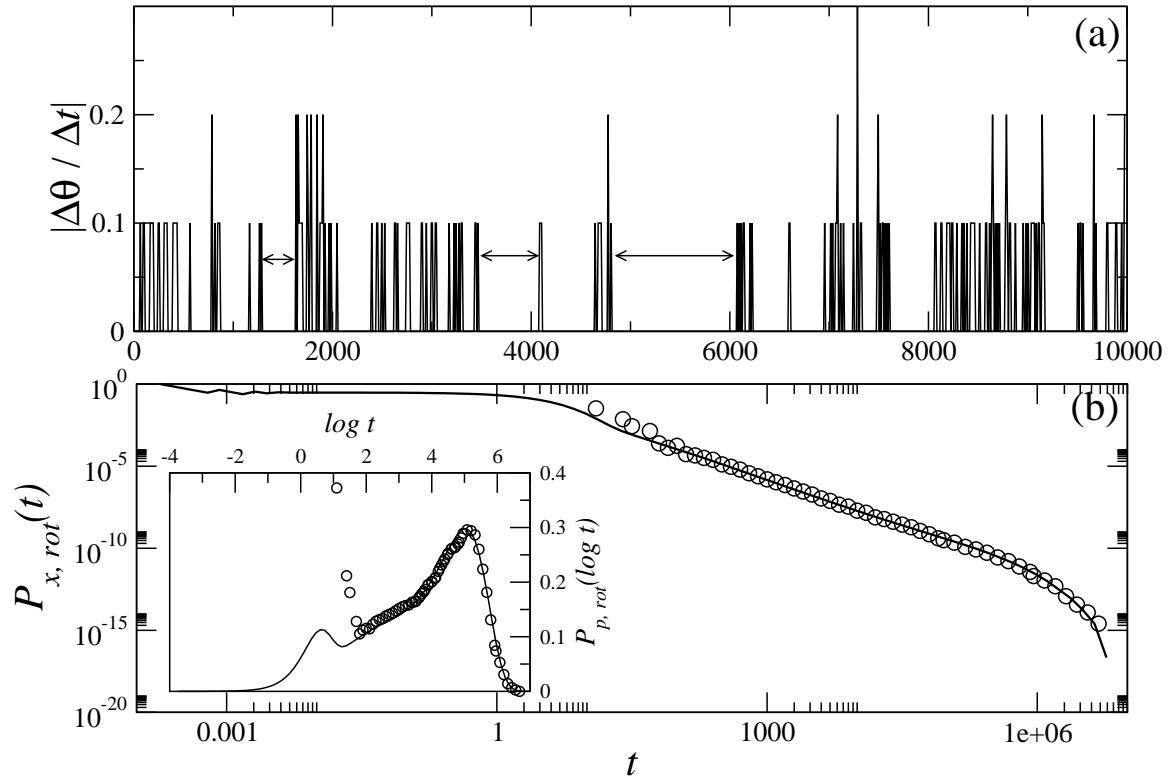


FIG. 5: (a) A plot of the absolute rate of angular change, $|\Delta\theta/\Delta t|$, for a rotational trajectory of a single particle at high density ($\rho = 0.75$). Three examples of exchange times are indicated by the double headed arrows. (b) Comparison of distributions of rotational exchange times obtained via data like those shown in panel (a) (open circles) and directly (solid line, see Fig. 4a, inset). The inset shows a comparison of the distribution of rotational persistence times. The values for the open circles in the inset are obtained by applying eqn. 1 to the the data in the main part of panel (b).

equation (1). The open circles are the results of direct calculations. We see that equation (1) is well-satisfied.

V. COMPARISON WITH EXPERIMENTS

Recent single molecule experiments determined distributions of rotational exchange times by following the dipole of embedded dye molecules [2, 3, 20]. Near the glass transition temperature, the absolute value of the rate of angular change, $|\Delta\theta/\Delta t|$, showed abrupt changes between different dynamical environments. We can anticipate from Fig. 1b that the same quantity in the rotational TLG will show similar behavior. From this quantity, Deschenes and Vandebout extracted a distribution of exchange times using a standard deviation criterion [3]. Here, we examine to what extent the distribution of times measured in this way corresponds to the distribution of rotational exchange times defined in section IV.

In Fig. 5a, we plot $|\Delta\theta/\Delta t|$ where $\Delta\theta = \theta(t + \Delta t) - \theta(t)$ for the rotational TLG at high density. Deschenes and Vandebout assigned an exchange event whenever the average angle jump changed by more than two standard deviations from the previous average angle jump. Due to the coarse grained nature of the rotational TLG, $|\Delta\theta/\Delta t|$ changes by discrete jumps. Therefore, exchange events can be unambiguously assigned whenever such a jump occurs. Fig. 5a plots $|\Delta\theta/\Delta t|$ in increments of ten sweeps during a portion of a single molecule trajectory. The fastest exchange event measurable at this time resolution is 10 sweeps. With infinite time resolution, however, we see that the definition of exchange times used in section IV would correspond precisely with the Deschenes-Vandebout procedure.

We verify this in Fig. 5b. Here, the distribution of times obtained via the Deschenes-Vandebout procedure outlined above (open circles) [21] are compared to the distribution of rotational exchange times calculated in section IV (solid line). The comparison is very good for about ten orders of magnitude. This method overestimates the distribution at early times for the reasons of time resolution mentioned in the previous paragraph. The inset shows a comparison of the distribution of rotational persistence times. The open circles are obtained from the open circles in the main panel of Fig. 5b via equation (1). Once again, the agreement is very good. In particular, the data obtained via the

procedure of Deschenes and Vandenbout captures the structure and location of the main peak.

Single molecule experiments also measured the mean rotational exchange times, $\tau_{x,rot}$ (i.e. the first moment of $P_{x,rot}(t)$, FIG. 4a, inset), as a function of temperature. It was found that $\tau_{x,rot}$ scaled with temperature in the same way as τ_r , the rotational correlation time, and that $\tau_{x,rot}$ was 10-20 times larger than τ_r at a given temperature [3, 20]. Our calculations indicate that $\tau_{x,rot} \sim (1-\rho)^{-2}$ or, using the definition that $1-\rho \equiv \exp(-1/T)$ [6], $\tau_{x,rot} \sim \exp(-2/T)$. The rotational correlation time, τ_r , scales like the structural relaxation time: $\ln \tau_r \sim \exp(1.7/T)$ [5, 6]. That is, $\tau_{x,rot}$ exhibits a much weaker dependence on temperature than τ_r similar to what is found in spin-facilitated models [19]. We also find that $\tau_{x,rot}$ is as much as six orders of magnitude times smaller than τ_r at the highest densities. This difference with experimental findings is most likely due to the issue of time resolution mentioned earlier and also discussed in [20] which biases experimental measures of $\tau_{x,rot}$ to longer times.

Acknowledgments

The author would like to acknowledge David Chandler, Juan Garrahan and Younjoon Jung for valuable discussions and the US National Science Foundation and Department of Energy (grant no. DE-FE-FG03-87ER13793) for funding. The author was an NSF graduate research fellow for part of this work.

-
- [1] M. D. Ediger, *Annu. Rev. Phys. Chem.* **51**, 99 (2000).
 - [2] L. A. Deschenes and D. A. V. Bout, *Science* **292**, 255 (2001).
 - [3] L. A. Deschenes and D. A. V. Bout, *J. Phys. Chem.* **105**, 11978 (2001).
 - [4] F. Ritort and P. Sollich, *Adv. Physics* **52**, 219 (2003).
 - [5] C. Toninelli, G. Biroli, and D. S. Fisher, *Phys. Rev. Lett.* **92**, 185504 (2004).
 - [6] A. C. Pan, J. P. Garrahan, and D. Chandler, *cond-mat/0410525* (2005).
 - [7] A. C. Pan, J. P. Garrahan, and D. Chandler, *Chem. Phys. Chem.* (2005), (in press).
 - [8] W. Kob and H. C. Andersen, *Phys. Rev. E* **48**, 4364 (1993).
 - [9] C. Donati and J. Jäckle, *J. Phys. Condens. Matter* **8**, 2733 (1996).
 - [10] J. Jäckle and A. Krönig, *J. Phys. Condens. Matter* **6**, 7633 (1994).
 - [11] A. Krönig and J. Jäckle, *J. Phys. Condens. Matter* **6**, 7655 (1994).
 - [12] The wavevector dependent quantity, $F_s(q, t)$, was conveniently calculated on the square lattice because a correspondence can be made between the reciprocal lattice vectors of the square and triangular lattices as in [10].
 - [13] M. E. J. Newman and G. T. Barkema, *Monte Carlo Methods in Statistical Physics* (Oxford University Press, 1999).
 - [14] Y. Jung, J. P. Garrahan, and D. Chandler, *Phys. Rev. E* **69**, 061205.1 (2004).
 - [15] L. Berthier, D. Chandler, and J. P. Garrahan, *Euro. Phys. Lett.* **69**, 320 (2005).
 - [16] S. F. Swallen, P. A. Bonvallet, R. J. McMahon, and M. D. Ediger, *Phys. Rev. Lett.* **90**, 015901 (2003).
 - [17] I. Chang, F. Fujara, G. H. B. Geil, T. Mangel, and H. Sillescu, *J. Non-Cryst. Solids* **172/174**, 248 (1994).
 - [18] L. Berthier and J. P. Garrahan, *Phys. Rev. E* **68**, 041201 (2003).
 - [19] Y. Jung, J. P. Garrahan, and D. Chandler, *cond-mat/0504535*.
 - [20] L. A. Deschenes and D. A. V. Bout, *J. Phys. Chem. B* **106**, 11438 (2002).
 - [21] The data shown by the open circles have been shifted vertically to facilitate comparison with the exact distribution of exchange times.